J Electroceram (2006) 16:351–355
DOI 10.1007/s10832-006-9878-0

Effects of Ni doping on B-site ordering and magnetic behaviors of double perovskite Sr_2FeMoO_6

Chen Li · Xue Junmin · John Wang

Abstract Sr_2FeMoO_6 of double perovskite structure has attracted much attention recently, owing to its substantial low-field magnetoresistance reported at room temperature. In our study, a mechanical activation process is devised for successful formation of Ni-doped double perovskite $Sr_2(Fe_{1-x}Ni_x)MoO_6$ ($0.00 \leq x \leq 0.20$). For the first time, a single phase of double perovskite is synthesized in air by using MoO_2 as the starting material. Ni doping in Sr_2FeMoO_6 significantly affects its long-range B-site ordering and magnetic behaviors, where the B-site long-range order parameter is progressively enhanced with increasing Ni doping level. Both magnetization and the Curie temperature in Sr_2FeMoO_6 are enhanced significantly by Ni doping, where they both depend almost linearly on the degree of B-site long-range ordering.

Keywords Sr_2FeMoO_6 · Double perovskite · B-site long-range order · Mechanical activation

1 Introduction

Low-field magnetoresistance together with a Curie temperature well above room temperature ($T_c \sim 415$ K) has been reported for double perovskite Sr_2FeMoO_6 [1], which stimulates renewed scientific interest in the double perovskites [2, 3]. Some of these compounds exhibit ferromagnetism and half-metallicity with a high spin polarization at the Fermi level, making them promising candidate materials for spintronics and several other technologically important applications.

The ideal structure of Sr_2FeMoO_6 consists of alternating FeO_6 and MoO_6 octahedra, where Fe^{3+} ($3d^5$, $S = 5/2$) cations at B′ sites are antiferromagnetically coupled to Mo^{5+} ($4d^1$, $S = 1/2$) occupying the B″ sites. The ordering of Fe and Mo cations at the octahedral B sites promotes the equilibrium reaction of $Fe^{3+} + Mo^{5+} = Fe^{2+} + Mo^{6+}$, where the itinerant down-spin electron from Mo cation is shared by both atoms [4]. Accordingly, the magnetization of Sr_2FeMoO_6 is critically dependant on the degree of Fe/Mo cation order among the B′/B″ sublattices. However, synthesis of such double perovskite phase would inevitably lead to a certain degree of anti-site disorder defects at B sites, whereby some Fe atoms are misplaced at the Mo sites and vice versa. The anti-site disorder defects can change or even destroy the B-site long-range order and therefore adversely affect not only the magnetization, but also the Curie temperature and magnetoresistance of Sr_2FeMoO_6 [4, 5]. Early Monte Carlo simulations predicted a linear reduction of saturation magnetization and Curie temperature as a function of the anti-site disorder [6].

In the past few years, great efforts have been devoted to tune the B-site cation order in Sr_2FeMoO_6. On the one hand, much work has been done to enhance the B-site order by optimizing various synthesis conditions, such as the heat treatment temperature [5, 7, 8] and time [7, 9]. On the other hand, cation substitution or doping at both A site [10–12] and B sites [13–16] have been attempted, in order to modify the B-site order and thus the physical properties of Sr_2FeMoO_6. Doping by La at A site was reported to raise the Curie temperature, but it affected the B-site order in such a way that both the saturation magnetization and magnetoresistance were dramatically reduced [11]. More recently, Sui et al. [17] observed that by doping with Al at B site, the degree of B-site

C. Li · X. Junmin · J. Wang (✉)
Department of Materials Science and Engineering, Faculty of Engineering National University of Singapore, Singapore 117576
e-mail: msewangj@nus.edu.sg

cation ordering as well as the low field magnetoresistance at low temperature in Sr_2FeMoO_6 were significantly enhanced. However, the resulting magnetization at both room temperature and Curie temperature were greatly reduced [15, 17]. To the best of our knowledge, no proper study has been reported so far for Ni doping in Sr_2FeMoO_6. In this paper, we report a study on the effects of Ni doping on the B-site long-range order and magnetic properties in Sr_2FeMoO_6.

2 Experimental

Polycrystalline $Sr_2(Fe_{1-x}Ni_x)MoO_6$ ($x = 0.0$–1.0) samples were prepared via mechanical activation route [18]. Appropriate amounts of the starting oxides SrO, Fe_2O_3, NiO and MoO_2 were mixed together, and then subjected to mechanical activation in a high energy shaker mill (Spex 8000 M) for 20 hours in air. The mechanically activated compositions were subsequently pressed into pellets and then heat-treated at 900°C ($x = 0.0$–1.0) or 1100°C ($x = 0.0$–0.2) for 3 hours in flowing Ar.

Phase development and crystal structure of the mechanically activated compositions and sintered $Sr_2(Fe_{1-x}Ni_x)MoO_6$ were examined using X-ray diffraction of CuK_α radiation operated at 40 kV and 40 mA (XRD, Bruker AXS D8Advance). The XRD profiles were further analyzed by means of the Rietveld refinement method using LPHM-Rietica program [19, 20]. Magnetization at room temperature was measured by using a vibrating sample magnetometer (VSM, Oxford Instruments). The temperature dependence of magnetization was studied by using a high temperature VSM (Lakeshore, Model 7400) over the temperature range of 300–500 K.

3 Results and discussion

Figure 1(a)shows the XRD patterns of the powder mixtures of SrO, Fe_2O_3, NiO and MoO_2 for $Sr_2(Fe_{1-x}Ni_x)MoO_6$, when subjected to mechanical activation for 20 hours in air. The double perovskite phase was well established with trace amounts of the starting material MoO_2, when Ni doping level x is less than 0.5 in $Sr_2(Fe_{1-x}Ni_x)MoO_6$. However, further increasing Ni doping level resulted in a new impurity phase of Sr_3MoO_6. Fig. 1(b) shows the XRD patterns of $Sr_2(Fe_{1-x}Ni_x)MoO_6$ upon heat-treatment at 900°C for 3 hours in flowing Ar. When Ni doping level is small ($x = 0$ and 0.1), a single phase of double perovskite $Sr_2(Fe_{1-x}Ni_x)MoO_6$was obtained. The impurity Sr_3MoO_6 phase appears when Ni doping level reaches 0.3, and it then increases notably with increasing Ni doping level. To synthesize Sr_2FeMoO_6, MoO_3 has commonly been used as the starting material. Therefore, a highly reducing atmosphere,

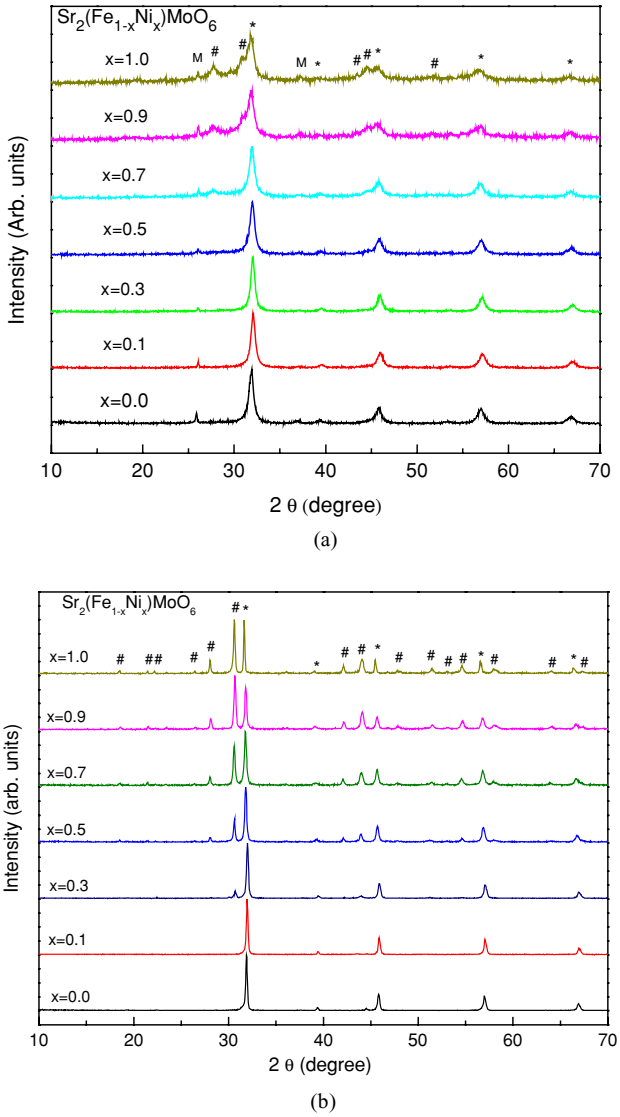

Fig. 1 (a) XRD patterns of mixed oxides of SrO, Fe_2O_3, NiO, and MoO_2 for $Sr_2(Fe_{1-x}Ni_x)MoO_6$, when subjected to 20 hours of mechanical activation in air. (b) XRD patterns of $Sr_2(Fe_{1-x}Ni_x)MoO_6$ ($x = 0.0$–1.0) derived from mechanical activation and then heat-treated in Ar at 900°C for 3 hours (*: Sr_2FeMoO_6 or Sr_2NiMoO_6, #: Sr_3MoO_6, M: MoO_2)

such as H_2, is always required to reduce Mo^{6+} to Mo^{5+}. In addition, the impurity $SrMoO_4$ phase can be easily formed in the process. For the first time, by using MoO_2 as the starting material and via the mechanical activation route, we have successfully synthesized the double perovskite phase in air, where Mo^{4+} was oxidized into Mo^{5+} during mechanical activation and formation of $SrMoO_4$ impurity was avoided.

Figure 2 plots magnetization versus applied field at room temperature for $Sr_2(Fe_{1-x}Ni_x)MoO_6$($x = 0.0$–1.0) derived from mechanical activation and subsequently heat-treated in Ar at 900°C for 3 hours. Interestingly, the magnetization increases with increasing level of Ni doping firstly, up to

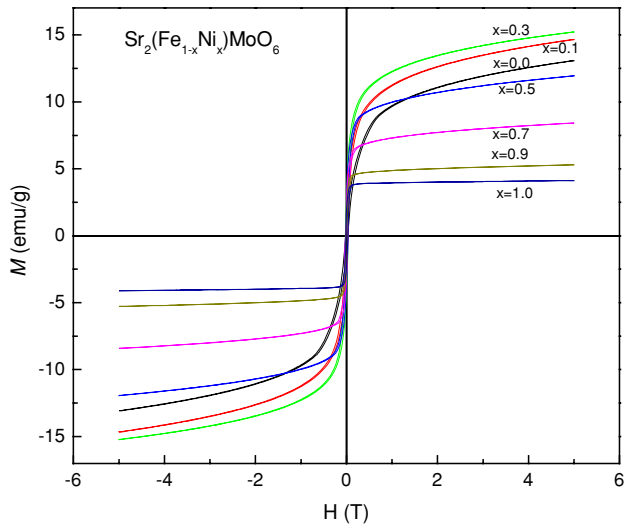

Fig. 2 Magnetic hysteresis loops at 290 K for $Sr_2(Fe_{1-x}Ni_x)MoO_6$ ($x = 0.0$–1.0) derived from mechanical activation and then heat-treated in Ar at 900°C for 3 hours

$x = 0.3$. When the Ni doping level further increases to 0.5, the magnetization decreases quickly with increasing level of Ni doping. The fall in magnetization is apparently due to the presence of the impurity phase, as has been confirmed by XRD phase analysis.

The XRD patterns for $Sr_2(Fe_{1-x}Ni_x)MoO_6$($x = 0.00$, 0.05, 0.10, 0.15, and 0.20), derived from 20 hours of mechanical activation and then heat-treated at 1100°C for 3 hours in Ar atmosphere, are shown in Fig. 3(a). They can be indexed to a tetragonal double perovskite structure, and show a series of superstructure reflections including (101) and (103), which characterize the long-range ordering of B′/B″ cations in the perovskite structure. The relative intensity ratio of the superstructure reflection (101) over the strongest (112)/(200) peak, $I_R = I_{101}/(I_{112} + I_{200})$, increases systematically when Ni doping level x increases from 0.0 to 0.2 (Fig. 3(b)), which indicates that the long-range order at B sites is progressively enhanced by an increasing level of Ni doping. To perform a detailed quantitative Rietveld analysis of the XRD profiles using LHPM-Rietica program [20], it can be assumed that all Ni ions occupy the Fe sites, by considering the large difference of ionic sizes between Ni^{2+} and Mo^{5+} (Mo^{5+}: 0.63 Å; Fe^{3+}: 0.65 Å; Ni^{2+}: 0.70 Å). The crystal structure is refined in the $I4/m$ space group [21], and the individual population parameters g of Fe (Ni) and Mo at the two B-cation sites are allowed to vary freely under the constraints that the overall occupancy of both sites is 100% and the amounts of Fe (Ni) and Mo cations are in the nominal 1:1 atomic ratio. The B-site long-range order parameter S can thus be defined by:

$$S = (g - F_{\mathrm{Mo}})/(1 - F_{\mathrm{Mo}}),$$

where g is the refined population parameter of Mo at the "right" Mo site and F_{Mo} is the atomic fraction of Mo among

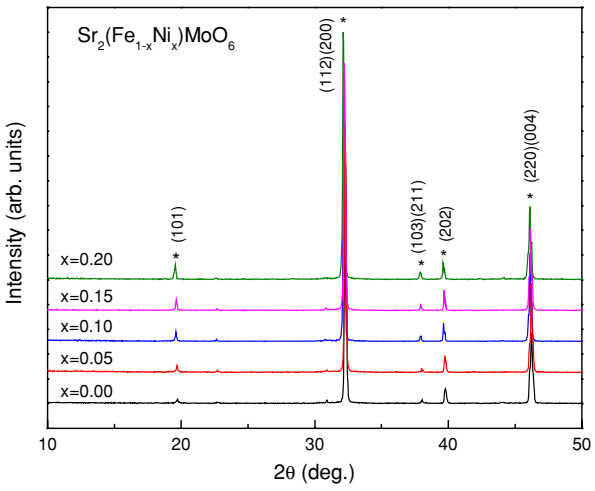

(a)

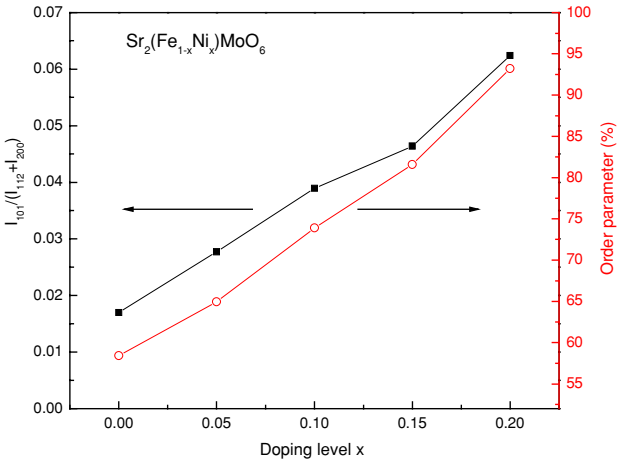

(b)

Fig. 3 (a) XRD patterns for $Sr_2(Fe_{1-x}Ni_x)MoO_6$ ($x = 0.0$–0.2) derived from mechanical activation and then heat-treated in Ar at 1100°C for 3 hours. (b) Left Y axis: dependence of the relative intensity ratio $I_{101}/(I_{112} + I_{200})$ on Ni doping level x; Right Y axis: B-site long-range order parameter S as a function of Ni doping level x

the B-site atoms ($F_{\mathrm{Mo}} = 0.5$ in the present case). In this notation, $S = 1.0$ and 0.5 corresponds to the perfectly ordered and completely disordered structures, respectively.

The long-range order parameter S of Fe (Ni) and Mo cations among the octahedral B sites is plotted in Fig. 3(b) (right Y axis) against Ni doping level x. In an agreement with the relative intensity ratio I_R, the long-range order parameter is enhanced significantly by Ni doping, from $S = 0.584$ for $x = 0$ to $S = 0.932$ for $x = 0.20$, and increases almost linearly with the level of Ni doping. The order-disorder transition of B cations in double perovskites $A_2B'B''O_6$ was previously addressed [22, 23]. One of the requirements for a long-range order is an enlarged difference in ionic size and valence between B′ and B″ cations. If the charge difference between B′ and B″ is greater than 2, a complete order occurs,

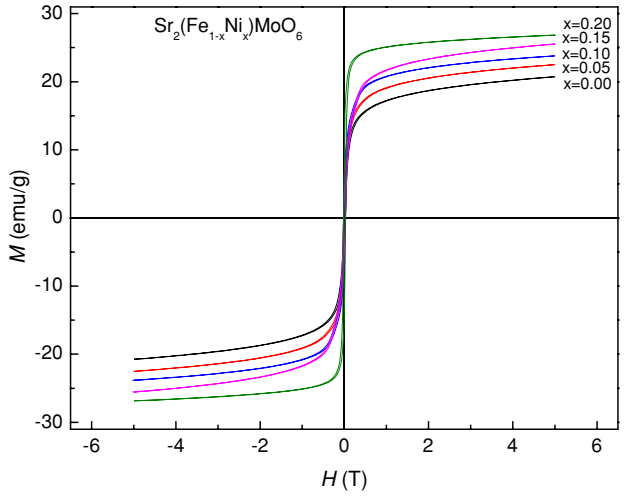

(a)

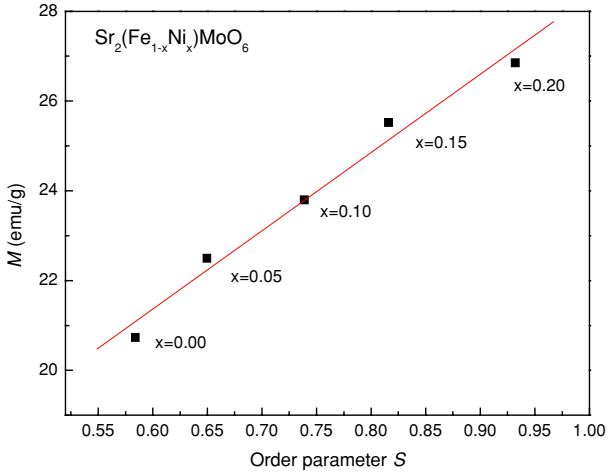

(b)

Fig. 4 (a) Magnetic hysteresis loops at 290 K for $Sr_2(Fe_{1-x}Ni_x)MoO_6$ ($x = 0.0$–0.2). (b) Dependence of magnetization on the B-site long-range order parameter S

for instance, in the $A_2B^{2+}B^{6+}O_6$ and $A_2B^{+}B^{7+}O_6$ type perovskites. As a matter of fact, the differences in cationic size and charge between Ni^{2+} and Mo^{5+} are larger than those between Fe^{3+} and Mo^{5+}. Therefore, substitution of Fe^{3+} by Ni^{2+} can undoubtedly facilitate the formation of an ordered structure.

Figure 4(a) shows the magnetization versus applied field curves for $Sr_2(Fe_{1-x}Ni_x)MoO_6$($x = 0.0-0.2$) measured at room temperature. Magnetization of $Sr_2(Fe_{1-x}Ni_x)MoO_6$ is systematically enhanced by an increasing level of Ni doping. As a comparison, B-site doping with other nonmagnetic elements such as Mn[14], Cr[16], Al[17] and V[24] all unfortunately reduced the room temperature magnetization of Sr_2FeMoO_6. Although Ni is ferromagnetic, the net magnetic moment of Ni^{2+} ($3d^8$, $S = 1$) is only 2 μ_B, which is much smaller than that of Fe^{3+} (5 μ_B). Therefore, the observed enhancement in magnetization for $Sr_2(Fe_{1-x}Ni_x)MoO_6$ cannot be accounted for by the magnetic nature of Ni itself. Indeed, the increase in magnetization implies that the strength of antiferromagnetic coupling between B′ and B″ sublattices is enhanced, which is apparently due to an increase in the degree of Fe (Ni) and Mo cation order among the B sites. The dependence of magnetization on the B-site long-range order parameter S is further plotted in Fig. 4(b), where the magnetization of $Sr_2(Fe_{1-x}Ni_x)MoO_6$ increases almost linearly with the increasing order parameter.

To further understand the doping effect of Ni in $Sr_2(Fe_{1-x}Ni_x)MoO_6$ ($0.00 \le x \le 0.20$), their Curie temperatures T_c were determined from the respective inflexion point of the magnetic transition by using the first numerical derivative dM/dT (Fig. 5(a)). As shown by the inset in Fig. 5(a), T_c is progressively raised by the increasing level of Ni doping,

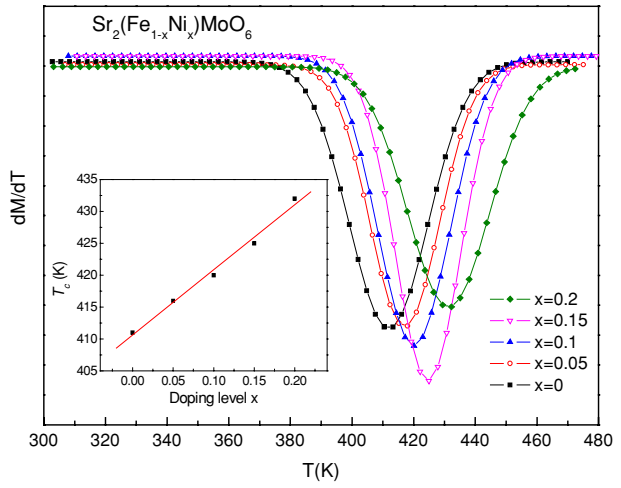

(a)

(b)

Fig. 5 (a) The derivative of magnetization as a function of temperature for $Sr_2(Fe_{1-x}Ni_x)MoO_6$ ($x = 0.0$–0.2). The inset shows the dependence of T_c on Ni doping level x. (b) Dependence of the Curie temperature on the B-site order parameter S. The line is a least-square linear fit

at a rate of about $d(T_c)/dx = 1$ K/% of Ni at the B site. The observed enhancement in the Curie temperature for Ni-doped Sr_2FeMoO_6 is in agreement with that has been discussed for Ni doping on the B-site cation order. In Fig. 5(b), the Curie temperature is further plotted against the B-site long-range order parameter S. Apparently, there is a linear correlation between the two parameters. The enhancement in T_c suggests that the average strength of magnetic interactions is reinforced by Ni doping, which is obviously related to an increase in the degree of B-site order. The linear correlation between the Curie temperature and the long-range order parameter S can be fitted quite nicely to $T_c = 376.9 + 59.4$ S (Fig. 5(b)), suggesting that the Curie temperature is raised by ~6 K when the long-range order parameter increases by 10%. Accordingly, the calculated T_c for the perfectly ordered crystal ($S = 1.0$) would be around 436 K, which agrees very well with the prediction of the theoretical model by Cai et al. [25]. In Ni-doped Sr_2FeMoO_6, Ni^{2+} not only affects the order at octahedral B sites but also mediates the valence equilibrium between Fe^{3+}/Fe^{2+} and Mo^{5+}/Mo^{6+}. Consequently, the electronic itinerancy of the minority-spin carriers from Mo cations is affected. As a result, the magnetic interactions in Sr_2FeMoO_6 are significantly reinforced by Ni doping, which raises both the magnetization and Curie temperature in Sr_2FeMoO_6.

4 Conclusions

$Sr_2(Fe_{1-x}Ni_x)MoO_6$ of double perovskite structure can be realized by mechanical activation of mixed oxides, where MoO_2 is used as the starting material. Too high a doping level of Ni (i.e., $x > 0.3$) results in occurrence of a minor amount of impurity phase. Ni doping significantly enhances the long-range order parameter S among octahedral B sites in Sr_2FeMoO_6, from $S = 0.584$ for $x = 0$ to $S = 0.932$ for $x = 0.20$. Consequently, magnetization of $Sr_2(Fe_{1-x}Ni_x)MoO_6$ ($x = 0.0$–0.2) is systematically enhanced, whereby a linear correlation is observed with the degree of B-site order. The Curie temperature of Sr_2FeMoO_6 is also raised dramatically by an increasing level of Ni doping, from $T_c = 411$ K for $x = 0$ to $T_c = 432$ K for $x = 0.20$, where it also shows a linear dependence on the B-site long-range order.

References

1. K.-I. Kobayashi, T. Kimura, H. Sawada, K. Terakura, and Y. Tokura, *Nature* (London), **395**, 667 (1998).
2. C.L. Yuan, S.G. Wang, W.H. Song, T. Yu, J.M. Dai, S.L. Ye, and Y.P. Sun, *Appl. Phys. Lett.*, **75**, 3853 (1999).
3. D.D. Sarma, P. Mahadevan, T.S. Dasgupta, S. Ray, and A. Kumar, *Phys. Rev. Lett.*, **85**, 2549 (2000).
4. M.G. Hernandez, J.L. Martinez, M.J. Martinez-lope, M.T. Casais, and J.A. Alonso, *Phys. Rev. Lett.*, **86**, 2443 (2001).
5. Ll. Bacells, J. Navarro, M. Bibes, A. Roig, B. Martinez, and J. Fontcuberta, *Appl. Phy. Lett.* **78**, 781 (2001).
6. A.S. Ogale, S.B. Ogale, R. Ramesh, and T. Venkatesan, *Appl. Phys. Lett.*, **75**, 537 (1999).
7. H. Sakuma, T. Taniyama, Y. Kitamoto, and Y. Yamazaki, *J. Appl. Phys.*, **93**, 2816 (2003).
8. J. Navarro, Ll. Balcells, F. Sandiumenge, M. Bibes, A. Roig, B. Martínez, and J. Fontcuberta, *J. Phys.: Condens. Matter*, **13**, 8481 (2001).
9. T. Shimada, J. Nakamura, T. Motohashi, H. Yamauchi, and M. Karppinen, *Chem. Mater.*, **15**, 4494 (2003).
10. J.B. Goodenough and R.I. Dass, *Int. J. Inorg. Mater.*, **2**, 3 (2000).
11. J. Navarro, C. Frontera, Ll. Balcells, B. Martinez, and J. Fontcuberta, *Phys. Rev. B*, **64**, 24111 (2001).
12. J. Navarro, J. Nogues, J.S. Munoz, and J. Fontcuberta, *Phys. Rev. B*, **67**, 174416 (2003).
13. C.L. Yuan, Y. Zhu, and P.P. Ong, *J. Appl. Phys.*, **91**, 4421 (2002).
14. Y. Moritomo, H. Kusuya, A. Machida, E. Nishibori, M. Takata, M. Sakata, and A. Nakamura, *J. Phys. Soc. Jap.*, **70**, 3182 (2001).
15. A. Pena, J. Gutierrez, L.M. Rodriguez-Martinez, J.M. Barandiaran, T. Hernandez, and T. Rojo, *J. Phys.: Condens. Matter*, **13**, L1 (2001).
16. X.M. Feng, G.H. Rao, G.Y. Liu, H.F. Yang, W.F. Liu, Z.W. Ouyang, and J.K. Liang, *Physica B*, **344**, 21 (2004).
17. Y. Sui, X.J. Wang, Z.N. Qian, J.G. Cheng, Z.G. Liu, J.P. Miao, Y. Li, W.H. Su, and C.K. Ong, *Appl. Phys. Lett.*, **85**, 269 (2004).
18. J. Wang, J.M. Xue, D.M. Wan, and B.K. Gan, *J. Solid State Chem.*, **154**, 321 (2000).
19. V.K. Pecharsky and P.Y. Zavalij, *Fundamentals of Powder Diffraction and Structural Characterization of Materials* (Kluwer Academic Publishers, Boston, 2003), Chap. 7.
20. B. Hunter, *Rietica—A Visual Rietveld Program*, International Union of Crystallography Commission on Powder Diffraction Newsletter No. 20 (Summer, 1998), http://www.rietica.org.
21. O. Chmaissem, R. Kruk, B. Dabrowski, D.E. Brown, X. Xiong, S. Kolesnik, J. D. Jorgensen, and C.W. Kimball, *Phys. Rev. B*, **62**, 14197 (2000).
22. D. Sanchez, J.A. Alonso, M. Garcia-Hernandez, M.J. Martinez-Lope, and J.L. Martinez, *Phys. Rev. B*, **65**, 104426 (2002).
23. P. Woodward, R-D. Hoffmann, and A.W. Sleight, *J. Mater. Res.*, **9**, 2118 (1994).
24. Q. Zhang, G.H. Rao, X.M. Feng, G.Y. Liu, Y.G. Xiao, Y. Zhang, and J.K. Liang, *Solid State Commun.*, **133**, 223 (2005).
25. T.Y. Cai and Z.Y. Li, *J. Phys.: Condens. Matter*, **16**, 3737 (2004).